

RAPID DISSIPATION OF PRIMORDIAL GAS FROM THE AU MICROSCOPII DEBRIS DISK

AKI ROBERGE,¹ ALYCIA J. WEINBERGER,¹ SETH REDFIELD,² AND PAUL D. FELDMAN³

Received 2005 February 2; accepted 2005 May 13; published 2005 June 1

ABSTRACT

The disk around AU Microscopii, an M1 star in the β Pictoris moving group, is extraordinarily well suited for comparison with the β Pic debris disk (type A5 V). We use far-UV absorption spectroscopy of AU Mic to probe its edge-on disk for small amounts of H₂, the primary constituent of gas giant planets. Our conservative upper limit on the line-of-sight H₂ column density is $1.7 \times 10^{19} \text{ cm}^{-2}$, which is 18.5 times lower than the limit obtained recently from nondetection of submillimeter CO emission by Liu et al. In addition, there is a hint of H₂ absorption at a column density an order of magnitude or more below our upper limit. The H₂-to-dust ratio in the AU Mic disk is less than 6:1, similar to that in the β Pic disk. This shows that the primordial gas has largely been dissipated in less than about 12 Myr for both disks, despite their very different stellar masses and luminosities. It is extremely difficult to form a giant planet around AU Mic with current core accretion scenarios in such a short time.

Subject headings: planetary systems: protoplanetary disks — stars: individual (HD 197481 = GJ 803 = AU Microscopii) — stars: low-mass, brown dwarfs

1. INTRODUCTION

A circumstellar (CS) disk around a young star evolves from a massive remnant of star formation (a primordial disk, composed mostly of H₂ gas) to a relatively low mass, gas-free planetary system. But there are difficulties reconciling observations of CS disks with current theories of giant-planet formation. In the traditional picture, giant planets form by accretion of gas onto a massive solid core, which must form before the primordial gas in the disk dissipates. Core formation takes at least a few million years for solar-type stars, much longer for lower mass stars (Laughlin et al. 2004). Observations suggest that the primordial gas dissipation timescale is shorter than about 10 Myr, possibly as short as 1 Myr in regions of high-mass star formation (Bally et al. 1998). With these short gas lifetimes, it would be fairly difficult to form giant planets with current core accretion scenarios around most solar-type stars, and extremely difficult around all low-mass stars.

However, giant planets have been found around many G- and K-type stars and two M-type stars (e.g., Butler et al. 2004). This has led some workers to suggest alternative theories for giant-planet formation, that is, that they form rapidly by direct collapse in gravitationally unstable disks (Boss 1998). But it is not clear that current core accretion models must be rejected, because of the uncertain timescale for primordial gas dissipation around stars of various masses in different star-forming environments. Comparison between the abundance of giant planets around M stars and the typical H₂ gas lifetime in their disks will be a powerful constraint on theories of giant-planet formation.

The M1 star AU Microscopii (GJ 803) has long been studied as a nearby flare star ($d = 9.94 \pm 0.13$ pc). It is comoving with the A5 V star β Pictoris, indicating they formed in the same region and are the same age (12_{-4}^{+8} Myr; Zuckerman et al. 2001).

The CS dust around AU Mic was imaged in reflected light and shown to lie in an edge-on disk (Kalas et al. 2004). This disk is uniquely suited for comparison with the β Pic debris disk and provides a valuable opportunity to examine the effect of stellar mass on disk evolution.

The inclination of the AU Mic disk within 50 AU of the star is less than 1° (Krist et al. 2005), even more edge-on than the β Pic disk ($i = 3^\circ$; Heap et al. 2000). CS gas in the β Pic disk has been observed with line-of-sight absorption spectroscopy (e.g., CO; Roberge et al. 2000), and a low upper limit on the H₂ abundance was set using far-UV absorption spectroscopy (Lecavelier des Etangs et al. 2001). This limit showed that the primordial gas has largely been dissipated. In this Letter, we apply a similar analysis to far-UV spectra of AU Mic, to probe sensitively for traces of primordial H₂ gas.

2. OBSERVATIONS

We used two sets of archival far-UV spectra of AU Mic, one each from the *Far Ultraviolet Spectroscopic Explorer* (*FUSE*) and the *Hubble Space Telescope* (*HST*) Space Telescope Imaging Spectrograph (STIS). Detailed descriptions of the data and analyses of the stellar emission lines may be found in Redfield et al. (2002) and Pagano et al. (2000). AU Mic was observed with *FUSE* on 2000 August 26 and 2001 October 10 for 17.3 ks and 26.5 ks, respectively. These spectra cover 905–1187 Å with a resolution of about 15 km s^{-1} ($R = \lambda/\Delta\lambda = 20,000 \pm 2000$). The data were recalibrated with CALFUSE version 2.4.0. The STIS data were taken 1998 September 6 (exposure time = 10.1 ks). These spectra cover 1170–1730 Å with a resolution of 4.4 km s^{-1} at 1350 Å ($R = 68,000$). We recalibrated the data with CALSTIS 2.17b.

Stellar flares occurred in both data sets. Since emission-line shapes and strengths can change during flares (e.g., Redfield et al. 2002), data taken at these times were excluded from our analysis. The *FUSE* bandpass is covered by eight partially overlapping spectra, two of which have the same zero-point wavelength offset (LiF1A and LiF1B). The bandpasses of the LiF1B *FUSE* spectrum and the STIS spectrum overlap, so we set the absolute wavelength calibration of the LiF1A and LiF1B spectra by cross-correlating on the C III $\lambda 1176$ stellar emission line

¹ Department of Terrestrial Magnetism, Carnegie Institution of Washington, 5241 Broad Branch Road, NW, Washington, DC 20015; akir@dtm.ciw.edu, alycia@dtm.ciw.edu.

² Harlan J. Smith Postdoctoral Fellow, McDonald Observatory, University of Texas at Austin, 1 University Station, C1400, Austin, TX 78712; sredfield@astro.as.utexas.edu.

³ Department of Physics and Astronomy, Johns Hopkins University, 3400 North Charles Street, Baltimore, MD 21218; pdf@pha.jhu.edu.

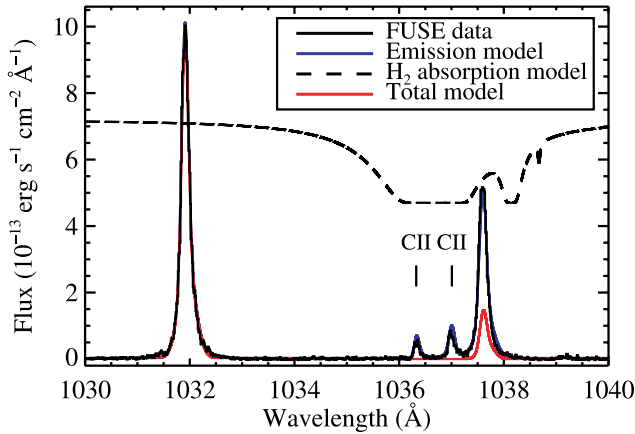


FIG. 1.—Portion of the *FUSE* LiF1A spectrum of AU Mic with a demonstration of the effect of line-of-sight H_2 absorption on the $\text{O VI } \lambda\lambda 1032, 1038$ and $\text{C II } \lambda\lambda 1036, 1037$ emission doublets. The intrinsic emission model, convolved with the *FUSE* LSF, is overplotted with a blue solid line. A convolved H_2 absorption model with the parameters of the upper limit from nondetection of submillimeter CO emission ($N_{\text{total}} = 3.15 \times 10^{20} \text{ cm}^{-2}$, $T = 40 \text{ K}$; Liu et al. 2004) is plotted with a black dashed line. For the H_2 model shown, we assumed unresolved lines and set the velocity of the gas to the stellar velocity ($v_* = -4.89 \text{ km s}^{-1}$). The total model is the absorption model multiplied by the emission model and then convolved with the *FUSE* LSF (red solid line). The $\text{O VI } \lambda 1032$ emission line is little affected by H_2 absorption, but such a large H_2 column density would dramatically suppress the $\text{O VI } \lambda 1038$ line and completely absorb both C II emission lines.

seen in both data sets. The zero-point offset of the *FUSE* spectra was small ($\approx 5 \text{ km s}^{-1}$).

3. ANALYSIS

Some of the many strong far-UV electronic transitions of H_2 overlap with commonly seen stellar emission lines, that is, the $\text{O VI } \lambda\lambda 1032, 1038$ doublet originating in the stellar transition zone and the chromospheric $\text{C II } \lambda\lambda 1036, 1037$ doublet. The portion of the *FUSE* LiF1A spectrum including these lines is shown in Figure 1. We have demonstrated that these emission lines can provide the background flux for absorption spectroscopy of H_2 (Roberge et al. 2001; Lecavelier des Etangs et al. 2001).

3.1. Creation of the Emission-Line Model

The first step in analyzing the *FUSE* spectra for molecular hydrogen absorption was to model the intrinsic flux in the emission lines. This is an emission model with infinite spectral resolution that will be multiplied by an intrinsic absorption model and then convolved with the instrumental line-spread function (LSF) to produce a model of the observed flux.

The $\text{O VI } \lambda 1032$ line is little affected by H_2 absorption, and the doublet lines are always in the optically thin ratio of 2:1, unless the $\lambda 1038$ line is suppressed by H_2 . The measured integrated flux ratio of the two O VI lines is 1.97 ± 0.19 , immediately indicating that there is little line-of-sight H_2 absorption. We began by least-squares fitting the sum of a narrow and a broad Gaussian to the $\lambda 1032$ line, since chromospheric and transition-zone emission lines from an active star such as AU Mic are not well fitted with single Gaussians (see, e.g., Redfield et al. 2002). The widths and peak intensities of the Gaussians were adjusted to remove the effect of the Gaussian *FUSE* LSF. The parameters from the fit to the $\lambda 1032$ line were used to model the $\lambda 1038$ line, with the peak flux set by the optically thin ratio.

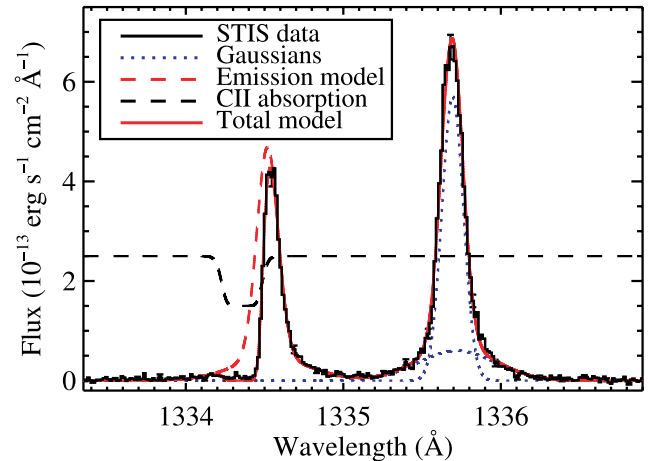


FIG. 2.—Portion of the E140M STIS spectrum of AU Mic showing the $\text{C II } \lambda 1335$ emission triplet (analyzed to aid in modeling of the *FUSE* C II emission lines). The blue wing of the $\text{C II } \lambda 1334.5$ line is cut off by line-of-sight C II absorption. The narrow and broad Gaussians from our modeling of the $\text{C II } \lambda 1335.7$ line are overplotted with blue dotted lines. The emission-line model of the triplet, convolved with the STIS LSF, is overplotted with a red dashed line. The convolved $\text{C II } \lambda 1334.5$ absorption model is plotted with a black dashed line. The total model is the absorption model multiplied by the emission model and then convolved with the STIS LSF (red solid line).

The $\text{C II } \lambda\lambda 1036, 1037$ doublet provides a tighter constraint on H_2 absorption, but the lines were difficult to model, since both can be affected. Therefore, we analyzed the $\text{C II } \lambda 1335$ triplet in the STIS data, shown in Figure 2. Examination of the line profiles shows that the blue wing of the $\lambda 1334.5$ emission line is cut off by ground-state C II absorption, which was initially identified as interstellar (IS), but the $\lambda 1335.7$ emission line is not affected by excited-state C II absorption.

We found the parameters of the C II emission by analysis of the $\lambda 1335.7$ line, which is blended with the weak $\lambda 1335.6$ line. The emission was modeled as the sum of a narrow and a broad Gaussian for each line, setting the line separation from the rest wavelengths. The relative line strengths were set using the products of the upper state multiplicities and Einstein A -coefficients. We then performed χ^2 minimization. The widths and peak intensities from this analysis were adjusted to remove the effect of the STIS LSF, which is very small since the lines are well resolved. The narrow component is at $v_n = -3.0 \pm 3.4 \text{ km s}^{-1}$, where the error bar is the $\pm 1 \sigma$ accuracy of the STIS wavelength calibration after a standard target acquisition (Pagano et al. 2000). Within the uncertainty, the C II emission is at the velocity of the star ($v_* = -4.89 \pm 0.02 \text{ km s}^{-1}$; Barrado y Navascués et al. 1999). As is usually the case, the broad component is slightly redshifted ($v_b = 3.0 \pm 3.4 \text{ km s}^{-1}$). The narrow component has $\text{FWHM} = 35.63 \pm 0.55 \text{ km s}^{-1}$, and the broad component has $\text{FWHM} = 129.4 \pm 3.9 \text{ km s}^{-1}$.

The parameters from the $\lambda 1335.7$ minimization were used to model the $\lambda 1334.5$ emission line, again setting the wavelength separation and relative line strength from the atomic data. We found that the $\lambda 1335.7$ line is not optically thin, since the peak intensities of the Gaussians in the $\lambda 1334.5$ line had to be increased slightly to fit the blue wing of the line. The emission model of the triplet convolved with the STIS LSF is shown with a red dashed line in Figure 2.

To find the parameters of the $\text{C II } \lambda 1334.5$ absorption, we used a Voigt intrinsic line profile to create an absorption model. A total model was made by multiplying the triplet emission model by the absorption model and then convolving the result

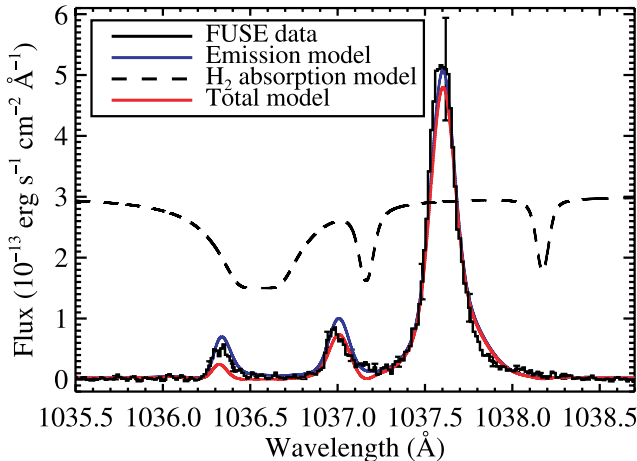


Fig. 3.—Upper limit on line-of-sight H₂ absorption toward AU Mic. The portion of the *FUSE* LiF1A spectrum near the C II $\lambda\lambda 1036, 1037$ doublet is shown, with the convolved emission model overplotted (blue solid line). The black dashed line shows the convolved upper limit H₂ absorption model [$N(J=0) = 1.6 \times 10^{19} \text{ cm}^{-2}$, $N(J=1) = 6.3 \times 10^{17} \text{ cm}^{-2}$]. The total model is the absorption model multiplied by the emission model and then convolved with the *FUSE* LSF (solid red line). For the H₂ model shown, the velocity was set to $+4.0 \text{ km s}^{-1}$. This is the most redshifted velocity expected for line-of-sight CS gas in Keplerian rotation in the edge-on disk, given the radial velocity of the star ($v_{\star} = -4.98 \text{ km s}^{-1}$) and the combined accuracy of the *FUSE* and STIS wavelength calibrations ($\pm 8.7 \text{ km s}^{-1}$). H₂ absorption models with velocities blueward of $+4.0 \text{ km s}^{-1}$ have an even more dramatic effect on the C II emission lines.

with the STIS LSF. The absorption parameters from χ^2 minimization of the total model are $N = 7.9_{-1.0}^{+1.9} \times 10^{14} \text{ cm}^{-2}$ (column density), $b = 17.50 \pm 0.63 \text{ km s}^{-1}$ (Doppler broadening parameter), and $v = -39.5 \pm 3.4 \text{ km s}^{-1}$. The convolved final model for the C II $\lambda 1335$ triplet is overplotted with a red solid line in Figure 2. The C II absorption is broad and blueshifted with respect to both the star and other absorption lines seen toward AU Mic (e.g., D I at $v = -21.7 \text{ km s}^{-1}$; Redfield & Linsky 2004). This suggests that the line-of-sight C II absorption may not be primarily IS.

Next, we modeled the C II emission doublet in the *FUSE* spectrum, using the velocities and widths of the narrow and broad Gaussians and the ratio of their peak intensities from the STIS analysis. The separation of the two lines and their relative strengths were calculated from the atomic data. The doublet emission model was multiplied by a C II $\lambda 1036$ absorption line, using the parameters given in the previous paragraph. The remaining free parameter was a scaling factor on the peak intensity of the $\lambda 1036$ line, which was determined by matching the model to the blue wing of the line. We found that the ratio of the line strengths calculated from the atomic data had to be adjusted slightly to fit the blue wing of the $\lambda 1037$ line, again indicating that it is not optically thin.

The C II and O VI models were added together to produce an infinite-resolution emission model for the 1030–1040 Å region of the *FUSE* spectrum. This model convolved with the *FUSE* LSF is plotted in Figure 1 with a blue solid line. One can immediately see that the C II emission lines in the *FUSE* data are slightly narrower than expected from the width of the STIS C II lines. There is no intrinsic reason for this, since we excluded flares from both data sets. Self-absorption suppresses the peak flux of an emission line but does not make it appear narrower. The emission lines are resolved, so the uncertainty in the spectral resolution of the *FUSE* data has little effect on the model. Other obvious *FUSE* instrumental or data artifacts

tend to make emission lines appear broader than they really are, not narrower. It seems there are only two ways to make the *FUSE* C II lines appear narrower than the STIS lines. The first is a calibration error that artificially broadened the STIS lines. There is such an error in STIS far-UV time-tag data (such as ours) retrieved from the archive before 2004 April 21.⁴ However, we recalibrated our data with the corrected pipeline software. The other way is to remove some emission from the *FUSE* lines with superposed H₂ absorption (discussed further in § 4.2).

3.2. Molecular Hydrogen Model Fitting

An H₂ absorption model was created using Voigt line profiles and molecular data from Abgrall et al. (1993). The free parameters were $N(J=0)$, the column density in the $\nu=0, J=0$ level; $N(J=1)$, the column density in the $\nu=0, J=1$ level; and v , the velocity of the gas. Only the two lowest energy levels were included, since they contain more than 90% of the molecules at the typical temperatures of debris disks ($< 200 \text{ K}$). The intrinsic width of any absorption is unknown, so we made the most conservative assumption (unresolved lines) and set the Doppler broadening parameter to be very small ($b = 1 \text{ km s}^{-1}$). The H₂ model was multiplied by the *FUSE* emission model and then convolved with the *FUSE* LSF. The resulting total model was compared with the data between 1035.5 and 1037.7 Å (the region most affected by H₂ absorption). To ensure that all local minima were found, χ^2 minimization was performed using very large ranges of parameters [$10^{12} \text{ cm}^{-2} \leq N(J=0)$ and $N(J=1) \leq 10^{22} \text{ cm}^{-2}$; $-60 \text{ km s}^{-1} \leq v \leq +60 \text{ km s}^{-1}$].

4. RESULTS

4.1. Upper Limits on H₂

Using our contours of χ^2 , we set upper limits on the line-of-sight H₂ column densities of $N(J=0) < 1.6 \times 10^{19} \text{ cm}^{-2}$ and $N(J=1) < 6.3 \times 10^{17} \text{ cm}^{-2}$. These column densities are ruled out at the $\geq 6 \sigma$ level for all v . In Figure 3, the convolved H₂ absorption model with these values is shown, and the total model is overplotted on the data near the C II lines. At lower column densities, the contours of χ^2 are complicated by the presence of a local minimum in addition to the absolute minimum, which is why we set the limits more conservatively from the 6σ contour rather than the typical 3σ contour. The upper limit on the total line-of-sight H₂ column density toward AU Mic is $N_{\text{total}} < 1.7 \times 10^{19} \text{ cm}^{-2}$; we did not assume a gas temperature to obtain this limit. If one assumes that the H₂ energy levels are thermally populated and fixes the gas temperature at any value below a few thousand kelvins, the total upper limit decreases.

From submillimeter observations, Liu et al. (2004) placed a 3σ upper limit on the CO column density in the AU Mic disk of $6.3 \times 10^{13} \text{ cm}^{-2}$, assuming any gas was in thermal equilibrium with the observed dust ($T = 40 \text{ K}$). Using a CO/H₂ ratio of 10^{-7} , this corresponds to a total H₂ column density of $6.3 \times 10^{20} \text{ cm}^{-2}$. The CO/H₂ value is unusually low compared with the typical IS value, since the authors tried to take into account the fact that the AU Mic disk is optically thin to interstellar UV photons. To convert this column density from emission observations to a line-of-sight absorption column, we divided the submillimeter upper limit by 2. This gives the lowest possible value, by assuming that the radial density dis-

⁴ See <http://www.stsci.edu/hst/stis/documents/newsletters/stan0412.html>.

tribution of the gas is extremely centrally peaked. Our χ^2 contours show that the submillimeter upper limit on the line-of-sight H_2 column density is ruled out at the greater than 20σ level for all v . Such a large column density would dramatically suppress the O νI $\lambda 1038$ emission line and completely obliterate both C II emission lines (see Fig. 1). Our upper limit in the previous paragraph is 18.5 times lower than the submillimeter upper limit, does not assume a gas temperature, and is free from the large uncertainties introduced by assuming a CO/H_2 ratio.

4.2. Possible Line-of-Sight H_2 Absorption

The fact that the *FUSE* C II emission lines are narrower than the STIS lines suggests there is a small amount of H_2 absorption toward AU Mic. The minimization with fixed b described above showed a second minimum in the χ^2 contours at H_2 column densities about an order of magnitude below our 6σ upper limits. In addition, there have been claims of weak fluorescent H_2 emission lines in the *FUSE* and STIS spectra (Pagano et al. 2000; Redfield et al. 2002); however, these lines are only detected at the $\approx 2\sigma$ level.

We attempted to detect line-of-sight H_2 absorption by performing χ^2 minimization with all parameters free, including b . These contours showed a minimum at large b and column densities a few orders of magnitude below the upper limits in § 4.1. But as before, there were multiple minima in the χ^2 contours, indicating there are multiple sets of parameters producing H_2 models that fit the data about equally well. Therefore, the model is overdetermined given the quality of the data. But taken at face value, our analysis indicates that the putative line-of-sight H_2 absorption is broad and blueshifted with respect to the star, as was the line-of-sight C II absorption in the STIS data.

5. DISCUSSION

Liu et al. (2004) measured a submillimeter dust mass of $0.011 M_\oplus$ within 70 AU of AU Mic. Their upper limit on the H_2 mass ($1.3 M_\oplus$) gives an upper limit on the H_2 -to-dust ratio of 118:1. Our limit on the line-of-sight H_2 column density

reduces the possible gas mass by at least a factor of 18.5, giving an upper limit on the H_2 -to-dust ratio of 6:1. The typical IS ratio is 100:1; therefore, the H_2 gas in the AU Mic disk has been depleted relative to the dust. The primordial gas is largely dissipated, and the gas lifetime was less than about 12 Myr.

Laughlin et al. (2004) showed that a core massive enough to gravitationally accrete a large gaseous envelope could not form within 10 Myr around a $0.4 M_\odot$ star. The only way current core accretion scenarios can form a giant planet around an M star is if its primordial gas survives much longer than about 10 Myr. Therefore, it is unlikely that a giant planet could form around AU Mic through these scenarios. There is indirect evidence of a giant planet around AU Mic, since the central region of the disk is cleared of dust grains (Liu et al. 2004) and the disk appears slightly warped in the *HST* Advanced Camera for Surveys scattered-light image (Krist et al. 2005). Central holes and warps have been attributed to the dynamical influence of an unseen giant planet.

We now consider the case of β Pic. The disk dust mass is $0.04 M_\oplus$ (Dent et al. 2000). Using the upper limit on the H_2 gas mass from *FUSE* ($\leq 0.1 M_\oplus$; Lecavelier des Etangs et al. 2001), the β Pic H_2 -to-dust ratio is less than 3:1, similar to the limit for AU Mic. This indicates that the primordial gas lifetimes in the two systems were both quite short, despite the very different stellar masses and luminosities ($L_{\text{AU Mic}} = 0.1 L_\odot$; $L_{\beta \text{ Pic}} = 8.7 L_\odot$). There is no O or B star in the β Pic moving group, so the short lifetimes are not easily explained by external irradiation. Given their spectral types, photoevaporation by the central stars seems unlikely to produce short gas lifetimes in both systems. Other possible dissipation mechanisms include stellar winds, magnetospheric accretion, and planet formation.

Our observation of broad, blueshifted line-of-sight C II absorption (and possibly H_2) would lead one to suspect that there is outflowing, low-ionization gas near the star, possibly in a stellar or disk wind. However, there may be an unusually large number of blended IS components at different redshifts along the sight line to AU Mic. We plan to investigate further by reexamining the putative fluorescent H_2 emission lines and all atomic absorption features in the STIS spectrum previously identified as interstellar.

REFERENCES

- Abgrall, H., Roueff, E., Launay, F., Roncin, J.-Y., & Subtil, J.-L. 1993, *A&AS*, 101, 273
 Bally, J., Testi, L., Sargent, A., & Carlstrom, J. 1998, *AJ*, 116, 854
 Barrado y Navascués, D., Stauffer, J. R., Song, I., & Caillault, J.-P. 1999, *ApJ*, 520, L123
 Boss, A. P. 1998, *ApJ*, 503, 923
 Butler, R. P., Vogt, S. S., Marcy, G. W., Fischer, D. A., Wright, J. T., Henry, G. W., Laughlin, G., & Lissauer, J. J. 2004, *ApJ*, 617, 580
 Dent, W. R. F., Walker, H. J., Holland, W. S., & Greaves, J. S. 2000, *MNRAS*, 314, 702
 Heap, S. R., Lindler, D. J., Lanz, T. M., Cornett, R. H., Hubeny, I., Maran, S. P., & Woodgate, B. 2000, *ApJ*, 539, 435
 Kalas, P., Liu, M. C., & Matthews, B. C. 2004, *Science*, 303, 1990
 Krist, J. E., et al. 2005, *AJ*, 129, 1008
 Laughlin, G., Bodenheimer, P., & Adams, F. C. 2004, *ApJ*, 612, L73
 Lecavelier des Etangs, A., et al. 2001, *Nature*, 412, 706
 Liu, M. C., Matthews, B. C., Williams, J. P., & Kalas, P. G. 2004, *ApJ*, 608, 526
 Pagano, I., Linsky, J. L., Carkner, L., Robinson, R. D., Woodgate, B., & Timothy, G. 2000, *ApJ*, 532, 497
 Redfield, S., & Linsky, J. L. 2004, *ApJ*, 602, 776
 Redfield, S., Linsky, J. L., Ake, T. B., Ayres, T. R., Dupree, A. K., Robinson, R. D., Wood, B. E., & Young, P. R. 2002, *ApJ*, 581, 626
 Roberge, A., Feldman, P. D., Lagrange, A. M., Vidal-Madjar, A., Ferlet, R., Jolly, A., Lemaire, J. L., & Rostas, F. 2000, *ApJ*, 538, 904
 Roberge, A., et al. 2001, *ApJ*, 551, L97
 Zuckerman, B., Song, I., Bessell, M. S., & Webb, R. A. 2001, *ApJ*, 562, L87